

## Research papers

# Adapting classical water quality diagrams for ecohydrological and policy applications

Paul Schot<sup>a,\*</sup>, Jack Beard<sup>b</sup>, Riki Hissink<sup>c</sup>, Michael Silberbauer<sup>d</sup>, Jasper Griffioen<sup>a,e</sup>

<sup>a</sup> Copernicus Institute of Sustainable Development, Utrecht University, Princetonlaan 8a, 3584 CB Utrecht, the Netherlands

<sup>b</sup> FutureWater, Wageningen, the Netherlands

<sup>c</sup> Blonk Sustainability Tools, Gouda, the Netherlands

<sup>d</sup> Formerly Department of Water and Sanitation, Pretoria, South Africa

<sup>e</sup> TNO Geological Survey of the Netherlands, Utrecht, the Netherlands

## ARTICLE INFO

## Keywords:

Ecohydrology  
Water quality diagram  
Nutrients  
Geohydrology  
Characterization  
Hydrochemistry

## ABSTRACT

Ecological values of water have gained increasing attention over the past decades in both (eco)hydrological research and water resources management. Water quality is an important ecological steering variable, and graphical water quality diagrams may aid in rapid interpretation of the hydrochemical status of a site. Traditionally used water quality diagrams for showing multiple variables (e.g. Stiff, Maucha) were developed primarily for hydrogeological purposes, with limited information on ecologically relevant nutrient parameters.

This paper presents adapted classical water quality diagrams that retain the traditional information on ions for hydrogeological characterization, and additionally provide information on nutrients for ecological water quality characterization.

A scaling factor is used for the minor ions to visually get them across more equally compared to the macro-ions in the water quality diagram. Scaling of minor ions is presented based on average concentrations, as well as on water quality policy norms. Four different water quality diagrams are presented, all with the same ions included, but with different appearances to suit different preferences of individual users. Regional, national and continental scale data are used to illustrate how the different diagrams show spatial and temporal water quality characteristics.

The adapted diagrams are innovative with respect to adding comprehensive visual information on the four ecohydrologically relevant nutrient species levels (NO<sub>3</sub>, NH<sub>4</sub>, PO<sub>4</sub>, K), advanced insight in redox status from the combination of four redox sensitive parameters (Fe, NO<sub>3</sub>, SO<sub>4</sub>, NH<sub>4</sub>) and the option to scale minor ions relative to average measured concentrations or to water quality policy norms. Using policy norms for scaling has the advantage of providing an ‘alarm function’ of exceedance of norms when concentrations surpass the ring used in the diagram. We discuss possible standardisation of scaling factors to enable comparability between sites.

## 1. Introduction

Over the past decades the importance of ecological values in water resources management has been steadily increasing. Growing populations, lack of sanitation and increased industrial and agricultural production have led to large-scale pollution of both surface water and groundwater (e.g. Millennium Ecosystem Assessment, 2005; Mateo-Sagasta et al., 2017). High concentrations of nutrients caused eutrophication of aquatic ecosystems leading to decreases in biodiversity and recreational values as well as economic damages (Cowx et al., 2010; Rosset et al., 2014; Dodds et al., 2009). From the 1970's onwards surface

water pollution gave rise to national legislation, especially in the USA and Europe. Also international treaties were being drafted in Europe to regulate water pollution of transboundary rivers, e.g. for the rivers Rhine (Dieperink, 2000) and Danube (Sommerwerk et al., 2010). This international cooperation culminated in the Water Framework Directive (WFD) of the European Union in 2000 (Directive, 2000), which aims for a ‘good status’ of water quantity, as well as chemical and ecological quality, for all groundwater and surface water in the EU. Especially the strong focus on ecological quality on the scale of the European Union was a novel aspect of this directive.

The increased attention for ecological values in water resources

\* Corresponding author at: Copernicus Institute of Sustainable Development, Utrecht University, Princetonlaan 8a, 3584 CB Utrecht, The Netherlands.

E-mail address: [p.p.schot@uu.nl](mailto:p.p.schot@uu.nl) (P. Schot).

<https://doi.org/10.1016/j.hydroa.2022.100137>

Received 16 September 2021; Received in revised form 25 August 2022; Accepted 1 September 2022

Available online 17 September 2022

2589-9155/© 2022 Published by Elsevier B.V. This is an open access article under the CC BY-NC-ND license (<http://creativecommons.org/licenses/by-nc-nd/4.0/>).

management was paralleled by an increased attention in scientific research on the interface between hydrology and ecology. This interdisciplinary field of ecohydrology is referred to by different names (e.g. ecohydrology; hydroecology) and definitions (Hannah et al., 2004). It is basically concerned with how hydrology steers ecological processes, and vice versa (Kundzewicz, 2002; Zalewski, 2000). Here we employ a broad interpretation of the term ecohydrology encompassing both aquatic and terrestrial ecology.

Ecohydrological site variables reflect the relation between the hydrologic cycle and ecological processes. It can be subdivided into a water availability part and a water quality part. Water availability is related to climate and topographical position in the landscape and steers selection of ecosystem communities adapted to different degrees of water stress (Porporato & Rodriguez-Iturbe, 2002). Water quality is related to geological setting, soil type, land use, composition of contributing water sources and local biogeochemical interactions between organisms, water, soil and atmosphere. Water quality steers selection of species mainly with respect to their tolerances for concentrations in salinity, acidity and nutrients (Herbert et al., 2015; Wassen et al., 1988; Ertsen et al., 1998). Determination and interpretation of water quality is notably complicated, as it may be defined by many different parameters, e.g. acidity, macro-ions, nutrients, trace elements, microorganics. These are often interlinked as they are subject to biogeochemical processes like oxidation, reduction, dissolution, precipitation, adsorption, cation exchange and complexation (Domenico & Schwartz, 1998; Appelo and Postma, 2004).

To facilitate interpretation of water quality measurements, graphical multi-parameter water quality diagrams may be useful. They enable transferring information on a number of selected parameters into visual water quality types summarizing the hydrochemical status of a site. Well known diagrams are those described by Stiff (1951), Piper (1944), Schoeller (1955), Collins (1923) and Maucha (1932), which all provide an overview of the main ions sodium (Na), chloride (Cl), calcium (Ca) or bicarbonate ( $\text{HCO}_3^-$ , actually often as alkalinity), magnesium (Mg) and sulfate ( $\text{SO}_4$ ). These diagrams have been applied for characterization of geological environments (Prol-Ledesma et al., 2004; Heikkinen et al., 2009), hydrochemical evolution and mixing processes (Cloutier et al., 2008; Kumar et al., 2006; Freeze and Cherry, 1979), effects of land use and water sources (Jeong, 2001; Schot and van der Wal, 1992), suitability for drinking water, agriculture and fen ecosystems (Yidana et al., 2010; Subramani et al., 2005; Silberbauer and King, 1991; Wassen et al., 1990) and water resources monitoring (Silberbauer, 2009; Frapporti et al., 1993).

Multi-parameter water quality diagrams in general have a twofold function. One is to determine the suitability of the water quality for a certain utilisation, e.g. for drinking water or vegetation communities. The other is to determine the origin and/or evolution of the water sampled at a certain location in relation to its flow path. The latter function may provide managers with information on the quality of the source water (e.g. infiltrating precipitation or surface water), alterations in water quality along the flow path due to biogeochemical processes, and possible changes in flow paths feeding a site, e.g. where groundwater seepage is replaced by infiltration of local precipitation (Van Loon et al., 2009; Schot et al., 2004). Such information provides reference points for conservation and restoration policies and measures, such as protection of water quality from pollution at the source or restoring groundwater seepage.

The shortcoming with currently most used water quality diagrams (e.g. Stiff, Piper, Maucha) is that they were developed primarily for hydrogeological purposes. Information is presented mainly on macro-ions like Na, Cl, Ca,  $\text{HCO}_3^-$ , Mg and  $\text{SO}_4$ . From this the major ecological steering factors salinity and acidity can be deduced using Na and Cl for salinity and Ca and  $\text{HCO}_3^-$  for alkalinity or acidity.

However, the existing diagrams lack adequate information on the third main ecological steering factor: nutrients. The nutrients nitrate ( $\text{NO}_3^-$ ) and potassium (K) are sometimes presented as single parameter,

potassium more often as the sum of Na + K. However, comprehensive nutrient information, notably on the pivotal nutrients nitrogen and phosphorus, is not commonly represented. This makes the diagrams unsuitable for evaluating primary ecologically relevant parameters and processes, or for comparing observed concentrations with water quality standards.

Some attempts have been made to design water quality diagrams specifically for ecohydrological use in relation to wetland vegetation. Van Wirdum (1991) developed the Ionic Ratio (IR) on the basis of calcium and chloride characterising water samples by their position relative to three main water types called *Atmotrophic* (precipitation), *Lithotrophic* (groundwater) and *Thalassotrophic* (seawater). Although widely used in especially Dutch ecohydrological literature, the method only provides a very general distinction for samples as a mixture of the three main water types. Remarkably, it does not provide any information on nutrients. Wassen et al. (1988) used an adapted Stiff diagram, with concentrations of nitrate ( $\text{NO}_3^-$ ), ammonium ( $\text{NH}_4^+$ ) and phosphate ( $\text{PO}_4$ ) presented as three additional separate lines below the diagram. However, characteristic shapes representative of certain water types are not easily discerned. Some authors added a nutrient parameter like  $\text{NO}_3^-$  to the classical water quality diagrams (e.g. Schot and van der Wal, 1992), but we found no water quality diagrams that encompass all the main eco(hydro)logically relevant nutrients  $\text{NO}_3^-$ ,  $\text{NH}_4^+$ ,  $\text{PO}_4$ , and K, despite the fact that a plea was made already in the early 1990's for an internationally applicable composite classification adapted to ecohydrological research (Pedroli, 1990).

We postulate that more ecohydrologically relevant water quality diagrams may aid the work of academic ecohydrologists and water and nature managers. Such diagrams on a map or timeline may provide rapid insight on ecohydrological and biogeochemical processes affecting water quality on a landscape scale, helping formulation of policies and measures for ecological and water quality conservation or restoration.

This paper aims to present ecohydrologically relevant water quality diagrams that provide information on both hydrogeological and ecological processes of interest to academic ecohydrologists and water and nature managers. We focus on freshwater systems as defined by chloride concentrations  $<300$  mg/l, thus including polluted freshwater, but excluding brackish and saline waters (cf. Stuyfzand, 1988; Griffioen et al., 2013).

## 2. Method

### 2.1. Selection of parameters

The selection of parameters for an ecohydrologically relevant water quality diagram was based on its envisaged ability to provide information on the following factors:

- Ecological site conditions, indicating the suitability of local water quality for flora and fauna development;
- Hydrological drivers of the site conditions on a landscape scale, providing indications on the origin of water sources replenishing the site, and on the processes driving water quality evolution along the flow path;

Selection was also directed to parameters which are commonly analysed in (eco)hydrological monitoring or research programmes such as macro-ions, nutrients and common metals.

The number of parameters to include in the diagram was kept as low as possible to keep the diagrams comprehensible, while still providing maximum relevant ecological and hydrological information. The selected parameters are detailed below (see Table 1).

- **Nutrients** are of prime importance for organisms but not included in commonly used water quality diagrams. We included  $\text{PO}_4$ ,  $\text{NO}_3^-$ ,  $\text{NH}_4^+$  and K in our water quality diagrams to enhance relevance for

**Table 1**  
Selected parameters for the ecohydrological water quality diagrams.

Parameter	Indicator value	Remarks
NO <sub>3</sub> , NH <sub>4</sub> , PO <sub>4</sub> , K	Nutrients Pollution	Of prime importance for organisms eq. in ecohydrology. NO <sub>3</sub> and NH <sub>4</sub> indicative for redox status.
Cl	Salinity Pollution	Conservative tracer indicating composition of principal water source, or mixing and pollution processes.
Ca	Acidity (indirect) Cation exchange Carbonate dissolution/ precipitation	Indirect indicator for acidity. Control on P-availability. Information about cation exchange in combination with other cations.
Fe	Reduction	Reduced environment often indicating organic matter availability, steering a.o. denitrification, sulfate reduction, methanogenesis, dissolution of heavy metals, and increased alkalinity. Control on P- and N-availability. Indicating saturated aquifer conditions.
SO <sub>4</sub>	Pollution Pyrite or gypsum dissolution Seawater	Influences internal eutrophication by phosphorus. Absence may indicate strongly reduced conditions.
Na	Salinity Pollution Cation exchange	Added for visual appearance. Information about cation exchange in combination with other cations, and feldspar dissolution.
HCO <sub>3</sub>	Alkalinity Carbonate dissolution/ precipitation Mineralisation of organic matter	Added for visual appearance. Indicator for silicate weathering. Indirect indicator for acidity.

ecohydrological studies. Both NO<sub>3</sub> and NH<sub>4</sub> are considered because these are the forms most present and analysed in water samples, they provide information on redox conditions, and they differ as to their availability to plants (Boudsocq et al., 2012).

- **Chloride** was selected as indicator of one of the primary water quality determinants for ecosystems being salinity (Herbert et al., 2015). Chloride is also a conservative ion not engaged in hydrochemical processes (except under hypersaline conditions; Appelo and Postma, 2004) and thus suitable as a natural tracer indicating the principal water source (e.g. precipitation, waste water, seawater), or mixing and pollution processes, when dissolution of rock salts is insignificant.
- **Calcium** was selected for multiple reasons. In most freshwater environments calcium is the main cation, which virtually always comes up in statistical analyses as a principal component explaining variance in water quality samples. Low calcium also functions as indirect indicator for relatively high natural acidity, e.g. in bogs where acidic precipitation recharges the organic soil devoid of calcium minerals (Gorham et al., 1985). Increasing calcium usually indicates decreasing acidity and increased alkalinity following dissolution of Ca carbonates along the flow path (Appelo and Postma, 2004). Calcium may further indicate agricultural pollution, or cation exchange following aquifer salinisation or freshening (Martínez and Bocanegra, 2002; Naus et al., 2019). Ecologically, calcium may be important by limiting phosphorus nutrient availability through precipitation of Ca phosphate minerals like hydroxyapatite (Griffioen, 2006; Dunne and Reddy, 2005) or complexation with Ca carbonates (Avnimelech, 1980).
- **Iron** dissolution is an indicator of reduced conditions at near-neutral and slightly alkaline pH (Drever, 1997; Appelo and Postma, 2004). Redox processes steer the concentrations of many ecohydrologically relevant parameters, e.g. nitrogen through denitrification and ammonification (Hefting et al., 2004), sulphate versus sulphite (Smolders et al., 2006) and (toxic) heavy metals through dissolution

(Borg et al., 2010). Reduction processes are commonly fueled by degradation of organic matter leading to increased alkalinity (Mattson and Likens, 1992). Iron may also control phosphorus nutrient availability through precipitation of iron Fe(II) phosphates (vivianite) and iron (hydr)oxides as sorbent (Gächter and Müller, 2003; House and Denison, 2002).

- **Sulfate** may indicate human pollution at the origin of the water sources, geohydrological processes like dissolution of sulfur bearing minerals (pyrite, gypsum), or mixing with seawater. In an ecological sense sulfate in wetlands may increase nutrient availability though oxidation of organic matter releasing ammonium and phosphate (Lamers et al., 1998; Smolders et al., 2006).
- **Sodium** was initially not selected as it does not add pivotal ecohydrological information and usually shows trends comparable to chloride, stemming from dissolution of halite rock salt (NaCl) or seawater as origin. It was nevertheless added to enhance comparability of the visual appearance of the adapted diagrams with existing diagrams which all show the major ion couple Na-Cl. As an added value sodium may indicate feldspar dissolution, while sodium/chloride ratios may indicate cation exchange processes related to e.g. salinisation and freshening of aquifers (Magaritz & Luzier, 1985; Appelo & Willemsen, 1987).
- **Bicarbonate** which may often be equalised to alkalinity was likewise only selected to enhance visual comparability with existing diagrams showing the major ions couple Ca-HCO<sub>3</sub>. Bicarbonate usually shows concentrations similar to calcium stemming from dissolution of Ca carbonates. It may have an added value by indicating silicate weathering and the occurrence of reduction processes manifested through increased bicarbonate concentrations following oxidation of organic matter. It also serves as an indirect indicator for acidity.

## 2.2. Definition of diagrams

### 2.2.1. Selection of diagram form

Initially we opted to present one adapted water quality diagram fit for ecohydrological studies. During our research it appeared personal preferences on diagram types may differ, so we decided to present a number of different diagrams, all using the same selected parameters. We started by using the Maucha and Stiff diagrams as a basis for adapted diagrams. Both show cations on the left, and anions on the right side of a vertical center line enabling insight in their mutual balance. The original Maucha diagram (Maucha, 1932) used the 4 anions CO<sub>3</sub>, HCO<sub>3</sub>, Cl, SO<sub>4</sub> (left) and the 4 cations K, Na, Ca, Mg (right). Stiff diagrams basically consist of 3 cations (usually Na, Ca, Mg) and 3 anions (usually Cl, HCO<sub>3</sub>, SO<sub>4</sub>), but many variations have been presented e.g. with 4 + 4 ions, changed ion sequence from top to bottom, or ion sums instead of a single ion (e.g. Na + K instead of Na).

We changed part of the above parameters to include all of our selected 10 parameters. We paired Na and Cl as main representatives for salinity, Ca and HCO<sub>3</sub> for carbonates and alkalinity (and indirect acidity) and Fe and SO<sub>4</sub> for information on redox conditions. Ammonium and NO<sub>3</sub> were paired as indicator of the redox status of the nutrient nitrogen. Potassium and PO<sub>4</sub> were paired to show the two remaining important nutrients, although they usually behave independently of each other, in contrast to the other 4 pairs. We defined two adapted diagrams based on the Maucha diagram and two on the Stiff diagram.

In the Maucha based diagrams we put the macro-ions at the bottom, Fe-SO<sub>4</sub> in the middle and the nutrients on top. The latter was intended to emphasize the nutrient information. We used the adapted Maucha diagram as described by Broch & Yake (1969) that allows for scaling of concentrations, with the length of the arrows indicating ionic concentrations. We call this form a Jester diagram. After some trials we felt the inward pointing arrows used for the minor concentrations in the (Maucha and) Jester diagram, presented a visually distorted view on the actual concentrations. We redesigned the diagram by using an arc starting from the diagram centre, delineating a surface area proportional

to the concentration. We call this form a Sector diagram.

In both diagrams a circle is used to indicate a standardised concentration per parameter, which will be explained in the next section. The ion pairs Na-Cl and Ca-HCO<sub>3</sub> are presented in different grey scales indicating a sort of basic reference (to salinity and alkalinity), while the other ions have distinct colours for emphasis.

In the Stiff based diagrams, we kept the top part presenting Na-Cl and Ca-HCO<sub>3</sub> to resemble the original Stiff diagram. Beneath these we added Fe-SO<sub>4</sub> followed by the nutrients at the bottom. We eliminated K from the Na row as in the original Stiff diagram, to express the nutrient K as a separate ecological relevant parameter. Both new Stiff based diagrams were developed with the top showing macro-ions, but differ with respect to the minor ions below. The Stiff-A diagram shows the minor ions separated by a small spacing from the macro-ions to emphasize the different individual scaling used for the minor ions (see next section). The Stiff-B diagram shows the minor ions depicted as separate bars similar to Wassen et al. (1988), but with broader bars and different colour for the minor ions. Both Stiff based diagrams present the classical macro-ions in grey scales and the minor ions in orange for emphasis. The length of the horizontal parameter axes are in meq/l, but with a scaling factor for Fe-SO<sub>4</sub> and the nutrients (see below).

### 2.2.2. Scaling of the minor ions

Essentially, the selected ions are considered equally important with respect to their information value. This implies they should come across in a visually balanced way in the diagram. With concentrations presented in meq/l, as done for most current water quality diagrams, this generally leads to overemphasis of the major ions Ca and HCO<sub>3</sub> (fresh systems) and/or Na and Cl (more brackish systems). To get all ions across visually more equal in the water quality diagram we introduced a scaling factor for each of the minor ions, consisting of Fe, SO<sub>4</sub> and the nutrients. A scaling factor is defined as the enlargement of concentrations of minor ions to get them displayed in the water quality diagram with comparable sizes to the macro-ions.

The range of concentrations of minor ions as found in natural groundwater was the basis for establishing a scaling of the different parameters. For this purpose a reference dataset was used consisting of over 6000 fresh groundwater analyses (Cl < 300 mg/l) from a well-studied 20\*25 km region in the Netherlands with many wetlands containing different water types, having varying degrees of salinity, acidity, redox conditions and nutrient concentrations (Schot & van der Wal, 1992). It appeared this reference dataset was useful as a basis for our scaling of the minor ions, at least for all examples (regional, national, continental, temporal) we present in this paper.

The major ions of fresh groundwater from the reference dataset showed median and average concentrations from 0.8 to 2.2 meq/l and 1.4–2.6 meq/l, respectively. To make the minor ions roughly comparable in size in the diagrams, we decided to scale the minor ions to 1 meq/l, meaning the average concentration of the ion in the dataset will plot equal to 1 meq/l.

The scaling factor for a minor ion X was defined as  $1/[\text{average concentration ion X}]$  of the dataset to be visualised. For an average minor ion concentration in the dataset used of e.g. 0.05 meq/l, the scaling factor becomes  $1/0.05 = 20$ , which will then plot at  $0.05 * 20 = 1$  meq/l in the diagram. A measured concentration of 0.1 meq/l would then be plotted as  $0.1 * 20 = 2$  meq/l in the diagram. In the Stiff type diagrams the meq/l are visualised by a scale bar above the diagram, with a vertical line indicating 1 meq/l as a reference for the scaled average concentration of the minor ions. In the Jester and Sector diagrams a circle is used that signifies 1 meq/l and denotes the average concentration of the minor ions. These 1 meq/l lines thus indicate whether the respective minor ion concentrations of a sample are below or above the average concentration in the dataset; they do not represent true concentrations but scaled, relative, concentrations. For the major ions the diagrams indicate the true concentration in meq/l.

For two of our examples (national scale and temporal variation) we

also used scaling of ions relative to particular water quality norms, not only for the minor ions but also for the major ions, since each ion may have an individual norm. The scaling factor in this case for parameter Y is defined as  $1/[\text{norm concentration for parameter Y}]$ . For example a NO<sub>3</sub> concentration of 60 mg/l relative to the European Union drinking water norm of 50 mg/l would be plotted as  $60 * 1/[50] = 1.2$ , which in the diagram would be visible as a length (Jester) or area (Sector) equal to 1.2 times the length/area for the norm of 50 mg/l, the latter which is defined as equal to 1 and indicated by a circle. In this way the diagram directly shows which parameters exceed the norm (length of parameter surpasses the circle indicating the norm). In this case all ions represent relative concentrations (relative to norm).

### 2.2.3. Evaluation of diagrams on spatial and temporal scales

We evaluated our approach for both spatial and temporal applications to demonstrate their wide applicability, for both groundwater and surface water. Selection of demonstration sites was based on 1) areas for which we had access to water quality databases containing the necessary 10 parameters, and 2) which have been described previously in peer-reviewed scientific papers so readers can look up specifics of each area when needed. We used groundwater data on 3 nested spatial scales, ranging from regional via national to continental, primarily based on access of the authors to suitable databases: *regional* scale data from a 20\*25 km area in the Netherlands, displaying a wide range of different water types from rainwater-like to brackish (Schot & van der Wal, 1992); *national* scale data of shallow groundwater down to 30 m in the Netherlands as described by Griffioen et al. (2013); *continental* scale data of European groundwater from Wendland et al. (2008). For a temporal application we used surface water data from the Vaal River in South Africa showing water type variation over a monitoring period from January to November 2004 (Silberbauer, 2009). For each of these databases, a different adapted diagram type is used to illustrate spatial and temporal variation in water quality, their relation to natural biogeochemical and human processes, and value for monitoring and policy development. Background information on the respective areas can be obtained from the papers cited above.

## 3. Results

### 3.1. The Stiff-A diagram (Regional scale)

The new *Stiff-A diagram* in Fig. 1 graphically presents the main groundwater quality types in the central part of the Netherlands as described by Schot and Van der Wal (1992). These groundwater types were determined by cluster analysis of a set of 1349 fresh groundwater samples (Cl < 300 mg/l) containing 12 different water quality variables, including the 10 used in our adapted diagrams. Flow directions and flow system boundaries indicated in Fig. 1 are based on extensive hydrological system analysis studies in the area a.o. using flow path modelling, isotope tracers and hydrochemical interpretation (Schot et al., 1988; Schot, 1990; Schot and Molenaar, 1992). The comprehensive diagrams allow for a detailed hydrogeological and ec hydrological interpretation.

Hydrogeologically, recharge by precipitation on the sandy ridge in the east is reflected in groundwater type A showing rather low HCO<sub>3</sub> and increased Na, Cl, Ca, SO<sub>4</sub>, NO<sub>3</sub> and K concentrations indicating pollution by human activities in agricultural and urban areas. Low Fe together with high NO<sub>3</sub> and SO<sub>4</sub> concentrations indicate the groundwater is still oxidic or suboxic. Further down the flow path groundwater types B and C indicate 1) less pollution as water down the stream line is older and less affected by pollution, 2) slightly increased Fe and NH<sub>4</sub> suggesting some reduction processes, 3) increasing HCO<sub>3</sub> from dissolution of carbonates and possibly redox processes.

At the river plain we observe three distinct types of groundwater. Type D is shallow groundwater stemming from local precipitation that passes the confining peat layer during recharge. It is relatively acidic and

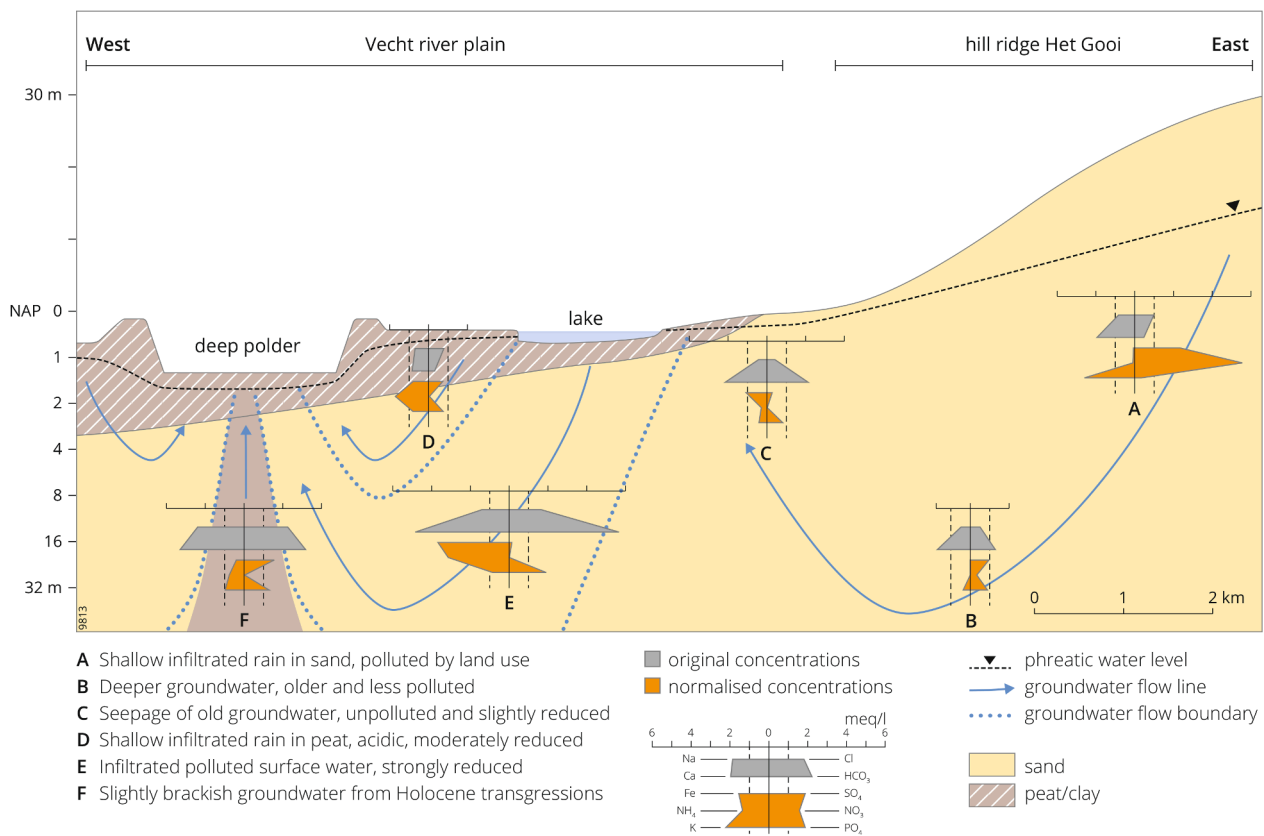


Fig. 1. Stiff-A diagrams showing groundwater types in the Central Netherlands (data derived from Schot and Van der Wal, 1992).

unpolluted and shows reduced conditions (Fe, NH<sub>4</sub>) common to peat layers and some K enrichment. Type E results from the infiltration of surface water in lakes and canals that have become polluted as a result of suppletion with River Rhine water during dry summer periods. Pollution signs are visible in the elevated Na and Cl and possibly PO<sub>4</sub> concentrations. High Fe and NH<sub>4</sub>, and low NO<sub>3</sub> and SO<sub>4</sub> concentrations indicate low redox potentials stemming from passage of the confining, largely saturated, peat or humic clay layers also leading to very high Ca and HCO<sub>3</sub> concentrations (Schot & Wassen, 1993). Type F stems from Holocene transgressions flooding the river plain with brackish-saline water, then infiltrating deep down into the main aquifer through density driven flow (Post, 2004). Due to mixing with fresh water in the aquifer the infiltrating water attains a decreased brackish character but still shows relatively high Na, Cl and SO<sub>4</sub>. These concentrations currently indicate upward flow of transgression affected water towards the surface in deep polders with low artificially controlled surface water levels (Schot and Molenaar, 1992).

Ecohydrologically, groundwater exfiltrating at the margin of the ridge (type C) is relevant. It has an unpolluted alkaline mesotrophic character, feeding protected so-called rich fens with high biodiversity, which include many rare and endangered plant species (Wassen et al., 1988). Conservation of this type of seepage is therefore a main aim of nature management. Type A indicates groundwater that is more recently infiltrated on the ridge and became polluted, which potentially may affect the rare rich fen plant communities in future when it exfiltrates. On the river plain, shallow peat water (type D) is also unpolluted and will likely become more alkaline during further flow providing favorable conditions for species rich fens when the water exfiltrates in adjacent lower lying polders, although nutrient concentrations (NH<sub>4</sub>, K) are somewhat higher than in groundwater originating from the ridge (Schot and Wassen, 1993). Types E and F are less suited for species rich fens due to their more saline and nutrient rich character.

### 3.2. The Jester diagram (National scale)

The **Jester diagram** in Fig. 2 presents main fresh (Cl < 300 mg/L) groundwater quality types in the Netherlands, as based on Griffioen et al. (2013). The Netherlands shows two distinctly different hydrogeological parts, roughly demarcated by the NE-SW directed mean sea level line in Fig. 2: a Pleistocene part in the east and south with thick phreatic aquifers consisting mainly of fluvial sands; and a Holocene part in the north, west and central riverine part with a confining top layer of predominantly clay and peat overlying Pleistocene sandy aquifers, and a coastal dune belt along the shore.

Fig. 2a shows major ions in grey in absolute concentrations in meq/l, while minor ions have been scaled relative to their average concentration over all areas. **Salinity** as indicated by Na and Cl concentrations is highest in areas I and II in the coastal marine influenced Holocene part in the west (note only fresh groundwater samples (Cl < 300 mg/l) were considered in this analysis). The higher Cl concentration for this fresh groundwater is due to mixing of fresh and saline groundwater as well as infiltration of river water with elevated Cl concentrations (Stuyfzand, 1993). Area I also shows highest SO<sub>4</sub> concentration pointing to the same origins (Griffioen et al., 2008). In the Pleistocene part, shallow groundwater typically originates from infiltration of rain and no marine influences are present in the shallow aquifers. This causes low Cl concentrations.

**Redox** conditions as indicated by Fe point to non-reduced conditions in the most elevated areas with deep groundwater tables (X, VI), and predominantly reduced conditions elsewhere despite extensive NO<sub>3</sub> in parts of the Netherlands. SO<sub>4</sub> concentrations are highest in the marine influenced area I, as well as in the southern sandy Pleistocene area VII and chalkstone area X which are subject to intense agricultural leaching of nitrates. In the subsurface denitrification takes place by pyrite dissolution giving rise to increased SO<sub>4</sub> and relatively low NO<sub>3</sub> concentrations (Van Beek and Puffelen, 1987; Zhang et al., 2009). This

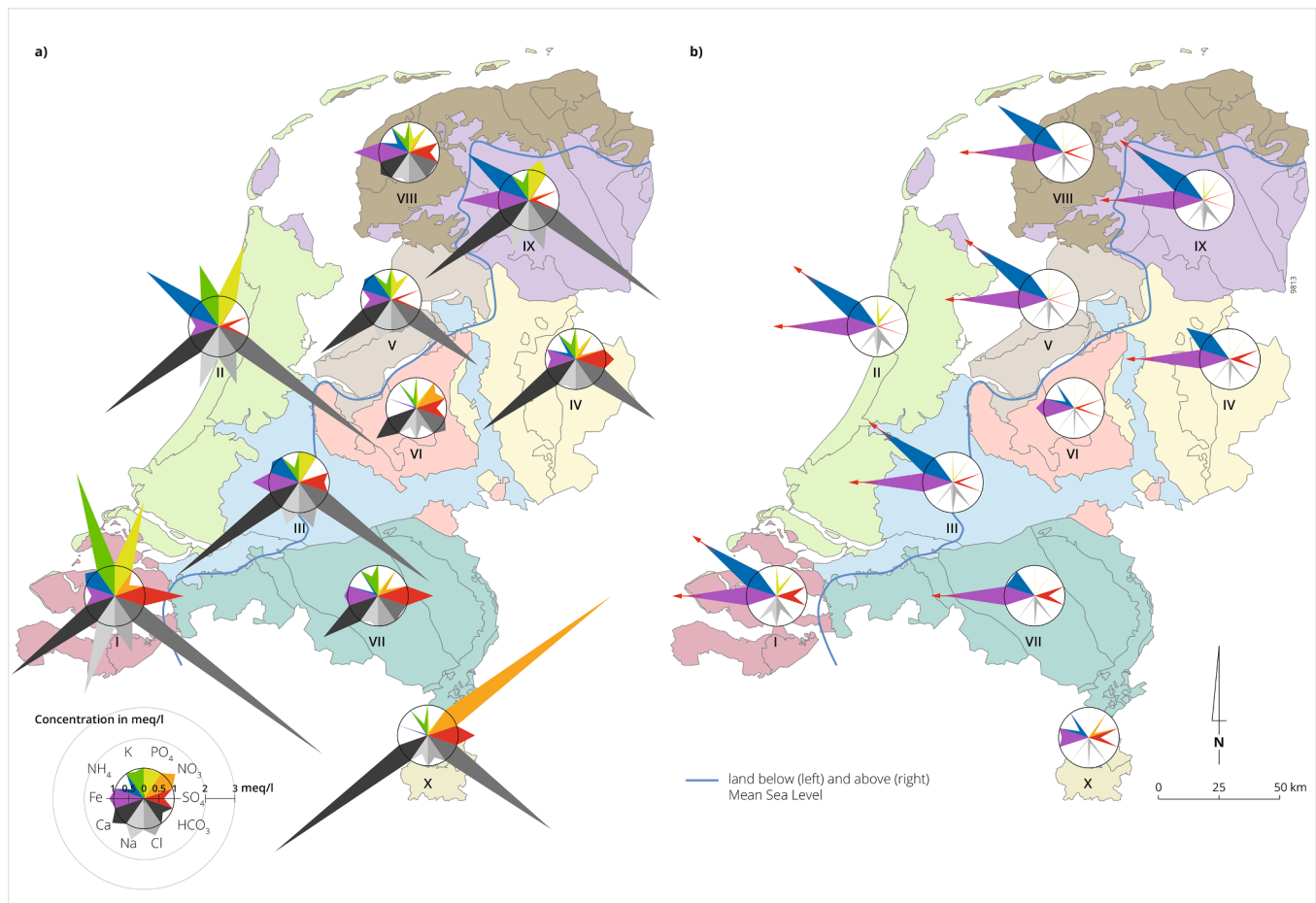


**Fig. 2.** Jester diagrams showing regionally averaged composition of fresh ( $Cl < 300$  mg/l) groundwater in the Netherlands. a) Minor ions scaled relative to their average concentrations over all regions; b) All ions scaled relative to drinking water norms in The Netherlands ([Drinkwaterbesluit, 2011](#); no norms for Ca,  $HCO_3$ , K). The rings indicate average (a) or norm (b) concentration. Red arrows in b) indicate concentration exceeds norm more than threefold. Classification of the coloured areas is based on geological and hydrogeological differences of the shallow subsurface (data based on [Griffioen et al., 2013](#)). (For interpretation of the references to colour in this figure legend, the reader is referred to the web version of this article.)

process does not take place in area X where  $NO_3$  remains high.

The newly added **nutrients** K and  $PO_4$  display highest concentrations in the western coastal areas I and II, while  $NH_4$  is highest in area II. These high nutrient concentrations have been linked to the degradation of marine sedimentary organic matter present in the Holocene confining top layer ([Mastrocicco et al., 2013](#); [Griffioen et al., 2013](#)). Nutrient  $NO_3$  is highest in area X where this agriculturally derived compound remains in an oxic state due to deep groundwater tables and absence of degradable organic matter in the chalkstone aquifer. Nitrate is low in the western part where the groundwater table is permanently close to the surface and the confining peat and clay layers provide degradable organic material for denitrification.

**Calcium and  $HCO_3$**  concentrations are highest in areas I, II, III and X pointing to dissolution of Ca carbonates from marine (I), lagoonal (II) and fluvial (III) sediments, and from chalkstone in the most southern part (X) and eventually Na- $HCO_3$  type groundwater in relation to freshening of saline aquifers with associated cation-exchange ([Appelo & Willemssen, 1987](#)). Areas I and II show relatively low Ca versus relatively high Na concentrations indicating Na- $HCO_3$  water types resulting from cation exchange processes, with Ca replacing Na from the cation-exchange complex that was formerly in equilibrium with Na-rich marine water.  $HCO_3$  increases upon cation-exchange due to enhanced Ca carbonate dissolution ([Griffioen et al., 2013](#)). Area X shows highest Ca concentrations related to chalkstone dissolution, but relatively low  $HCO_3$  with high  $NO_3$  and  $SO_4$  contributing significantly to total anion concentrations. The diagrams and their differences also confirm that the

geochemical control is stronger than the anthropogenic control despite large contamination of infiltrating rain and river water due to intensive agricultural and industrial activities in the Netherlands ([Van den Brink et al., 2007](#)).

The Jester diagrams make clear a number of issues not well known to most water managers and ecohydrologists, such as the naturally high nutrient concentrations (K,  $PO_4$ ,  $NH_4$ ) in the coastal areas. Likewise high  $NO_3$  leaching from intense agriculture in the eastern Pleistocene areas is well known, but less known is that by far the highest concentrations are in the southern chalkstone area due to lack of denitrification capacity, while pyrite dissolution (shown by high  $SO_4$ ) denitrifies groundwater to a considerable extent in areas VII and IV. Also less known is the predominantly reduced character of shallow groundwater in the northern area IX and VIII as evidenced by presence of dissolved Fe.

When concentrations are plotted relative to drinking water health norms ([Fig. 2b](#)) it becomes clear that Fe and  $NH_4$  are above drinking water norms in most of the areas. This would entail treatment before the water can be used for drinking water.

### 3.3. The Stiff-B diagram (Continental scale)

The new **Stiff-B diagram** is demonstrated for a selected number of major groundwater composition types at European scale ([Fig. 3](#)). The diagrams are based on the paper by [Wendland et al. \(2008\)](#) who made a European aquifer typology as a practical framework to assess major groundwater composition at continental scale. The typology included

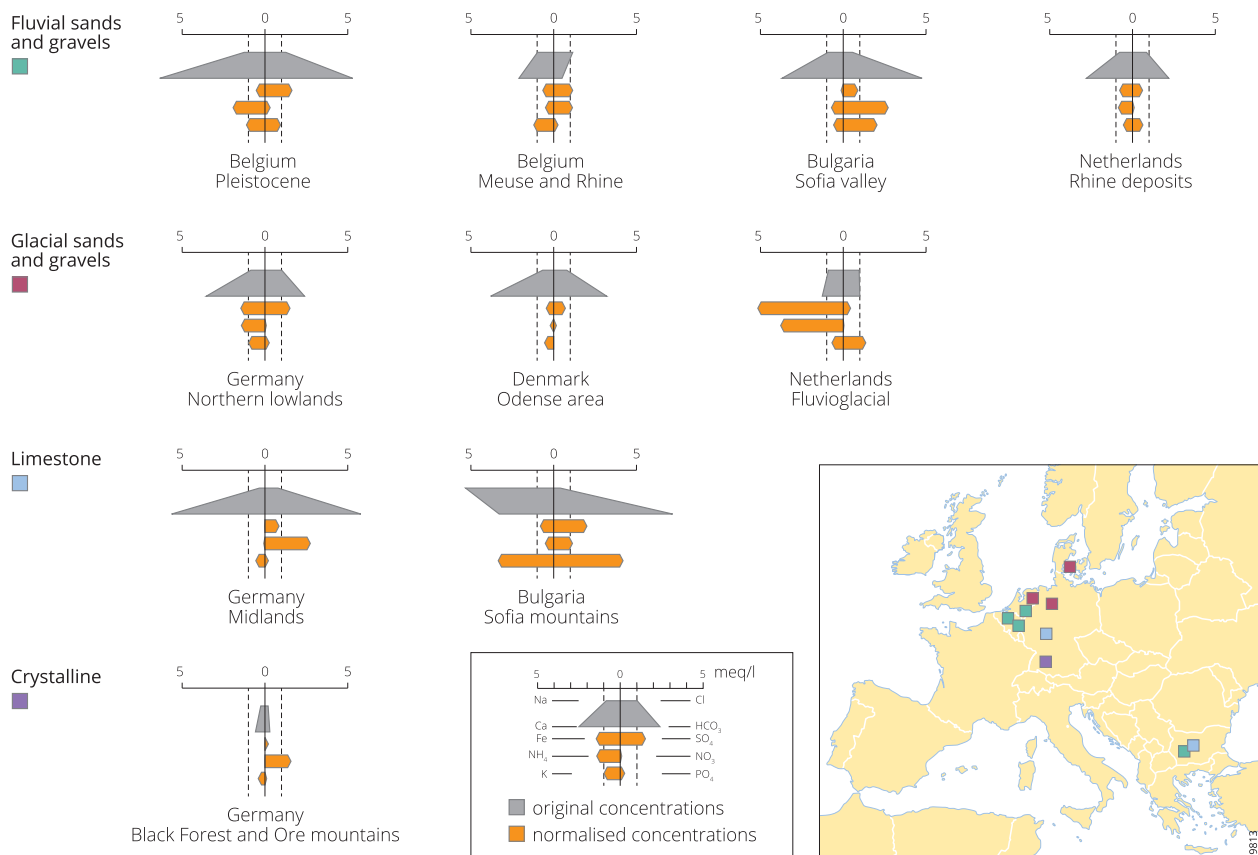


Fig. 3. Stiff-B diagrams illustrating groundwater composition for major aquifer types at European scale (data derived from Wendland et al., 2008).

major classes of aquifers with comparable petrographic properties. The various classes were expected to show similar groundwater compositions in comparable hydrodynamical and hydrogeological conditions. Major groundwater compositions were determined for aquifer types Sands and Gravels (with subtypes), Limestones and Crystalline Rocks. In the original paper results on groundwater compositions for each type were shown in the form of (extensive) tables covering 2.5 pages. This hampers quick comparison between different types. We therefore selected a number of groundwater composition types and plotted them using our new Stiff-B diagram to enable more rapid visual comparison (Fig. 3). For clarity we only plotted a limited number of types for the Sands and Gravels 7 out of 10), Limestones (2 out of 4) and Crystalline Rocks (1 out of 2).

The diagrams indicate that groundwater composition varies across Europe for similar aquifer types. For the **Fluvial** Sands and Gravels salinity is quite comparable, whereas differences are visible for Ca and HCO<sub>3</sub> in the order of a factor 3 and 10, respectively. Nitrate and phosphate are above average in Bulgaria Sofia Valley, while ammonium is highest in Belgium Pleistocene. The **Glacial** Sands and Gravels show relatively low Ca and HCO<sub>3</sub> and high Fe and NH<sub>4</sub> concentrations in Netherlands Fluvioglacial deposits compared to Denmark Odense area and Germany Northern Lowlands. **Limestone** in Bulgaria Sofia Mountains shows a NaCa-HCO<sub>3</sub> water type with high K and PO<sub>4</sub> concentrations, differing significantly from Germany Midlands. **Crystalline** Rocks groundwater from Germany Black Forest and Ore Mountains clearly shows lowest mineralization of all groundwater types.

The diagrams of Fig. 3 indicate that, contrary to the assumption of Wendland et al. (2008), groundwater composition in aquifers from the same typology may differ considerably between and within different countries, notably in redox conditions as well as alkalinity concentration, depending on regional petrographic and hydrogeological conditions. It is also apparent that in different geological settings the newly

added nutrient parameters may differ significantly, thus adding significant ecohydrological water quality information.

### 3.4. The Sector diagram (Temporal scale)

Fig. 4a presents changes in surface water quality in the form of Sector diagrams over the period Jan-Nov 2004 at an ambient water quality monitoring site of the Department of Water and Sanitation on the Rietspruit River, South Africa. The Rietspruit River is a tributary of the Vaal River in Gauteng province. Land use types in the Rietspruit catchment include gold mines, dryland agriculture, and high density residential (Silberbauer and Moolman, 1993; Showalter et al., 2000).

The changes in water quality during 2004 reflect pollution sources that include acid mine drainage (SO<sub>4</sub>) (e.g. Silberbauer, 2011) and treated sewage (Cl, PO<sub>4</sub>, NO<sub>3</sub> and NH<sub>4</sub>) (Dzwauro and Otieno, 2014). Summer rainfall in January to April appears to dilute the pollutant load; concentrations then increase in the dry months, until the rains begin again in late August or September.

Fig. 4b displays all ions relative to a set of norms based on values for “good quality” water in the South African Water Quality Guidelines (DWAF, 1996) and the prescribed Resource Quality Objectives (DWS, 2016) for this part of the Upper Vaal catchment. Fig. 4b makes clear that PO<sub>4</sub> concentrations exceed the norm set by water quality guidelines more than threefold in every sample, suggesting a constant source of (partly) untreated effluent may have been entering the Rietspruit. From January to April NH<sub>4</sub> is low and NO<sub>3</sub> is high, while from August till November this somewhat reverses to low NO<sub>3</sub> and high NH<sub>4</sub>, the latter also exceeding the norm. Whether this is related to changes in nutrient inputs or to oxygen concentrations in the water is not clear from the data measured by DWS. Changes in Fe concentration between rainy and dry periods may be related to runoff from mines lowering the pH, which increases the solubility of metal ions.

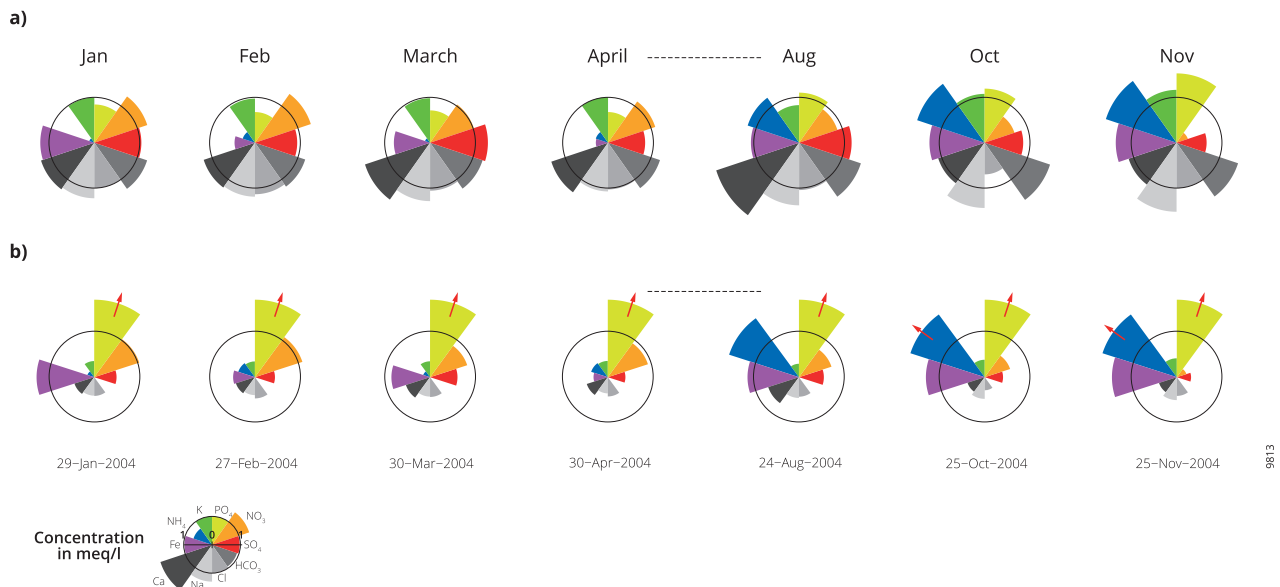


**Fig. 4.** Sector diagrams showing Jan-Nov 2004 changes in surface water quality of Rietspruit river in the Vaal catchment, South Africa (data from Department of Water and Sanitation, South Africa). a) Minor ions scaled relative to their average concentrations over all samples; b) All ions scaled relative to water quality guidelines (DWAF, 1996; DWS, 2016). The rings indicate average (a) or norm (b) concentration. Red arrows in b) indicate concentration exceeds norm more than threefold. (For interpretation of the references to colour in this figure legend, the reader is referred to the web version of this article.)

Generally, the addition of nutrients to the diagrams in both figures provide insights that go clearly beyond those obtained from classical diagrams restricted to major ions, notably since the nutrients are the prominent parameters exceeding water quality policy guidelines.

### 3.5. Intercomparison of adapted diagrams

Fig. 5 presents a comparison of the 4 adapted water quality diagrams for a number of samples taken from the four datasets used. The figure shows how identical samples lead to visually distinctly different diagrams. Showing the different diagrams to colleagues during the preparation of this paper indicated that the favored diagram differs between people, and may even differ between studied areas showing relatively low or relatively high salinity, carbonates or minor ions. Since there is apparently no one-size-fits-all diagram we present all 4 diagrams, so readers can decide themselves which type suits their needs best.

The Maucha based diagrams have macro-ions at the bottom, while the Stiff based diagrams have macro-ions at the top. Colouring in the Jester and Sector is much more pronounced than the two colours of the Stiff-A and -B. Also, the Jester diagram may become quite 'spiky' and take considerable plotting space when individual concentrations become relatively high. The Sector appears somewhat more compact. The Stiff based diagrams are characterized mainly by their typical grey and orange appearances.

## 4. Discussion

Four adapted water quality diagrams have been presented and demonstrated on both spatial (regional, national, continental) and temporal scales. The Regional example showed how the additional ions allow for a more profound ecohydrological analysis, leading to insights in redox processes in water infiltrating through the peat/clay layer on the river plain and (to a lesser extent) in deeper groundwater in the sandy hill ridge. For nature conservation, helpful insight is provided in possible nutrient pollution to seepage dependent fens at the ridge edge (by  $\text{NO}_3$ ), or to polders on the river plain (by  $\text{NH}_4$  and K). The National example provided new insight in high  $\text{PO}_4$ ,  $\text{NH}_4$  and/or K nutrient concentrations in the coastal regions, as well as in exceptionally high  $\text{NO}_3$  concentrations in the southern chalkstone area due to lack of

denitrification capacity. The Continental example made clear similar aquifer types not necessarily present similar water qualities as was postulated, and may differ considerably in nutrient concentrations depending on local human activities or (possibly) minor geological differences. The Temporal example of Vaal river water in South Africa showed high  $\text{PO}_4$  concentrations consistently surpassing water quality standards more than threefold, as well as possible seasonal differences in high  $\text{NO}_3$  and  $\text{NH}_4$  and Fe concentrations.

Scaling concentrations relative to water quality policy guidelines proved useful for quick visual insight in exceedance of norms relevant for the areas at stake.

Since water quality is a function of many parameters, the adapted diagrams with 10 parameters now provide a user friendly visual presentation enabling a more holistic analysis of hydrogeological and ecological processes of interest to ecohydrologists and water and nature managers.

With respect to hydrogeological processes the information value of the existing and commonly used Stiff and Maucha diagrams is retained. All major anions used in the classical diagrams ( $\text{Cl}$ ,  $\text{HCO}_3$ ,  $\text{SO}_4$ ) are also included in the adapted diagrams. For the cations, Na and Ca have been retained, while K is displayed as a separate value, whereas the classical Stiff and Piper diagrams display K as the sum of  $\text{Na} + \text{K}$ . The concentration of Mg has been left out of the new diagrams as this was considered less important from an ecohydrological perspective. This may be seen as a drawback when hardness or Mg itself is of significant interest for example in seawater intrusion processes with cation exchange. However, our parameter Ca is also roughly indicative of total hardness as well as in cation exchange processes following seawater intrusion. Instead Fe has been added as an important indicator of reduced hydrochemical conditions, as redox conditions are strongly steering concentrations of many water quality variables by means of hydrochemical processes.

By adding the nutrients, of which  $\text{NO}_3$  and  $\text{NH}_4$  are particularly redox sensitive, more advanced insight in redox conditions is offered by mutually comparing concentrations of Fe,  $\text{NO}_3$ ,  $\text{SO}_4$  and  $\text{NH}_4$ .

With respect to ecological processes the adapted diagrams add considerable extra information compared to classical water quality diagrams. They present comprehensive information on the four most common environmental nutrients: both nitrogen compounds  $\text{NO}_3$  and



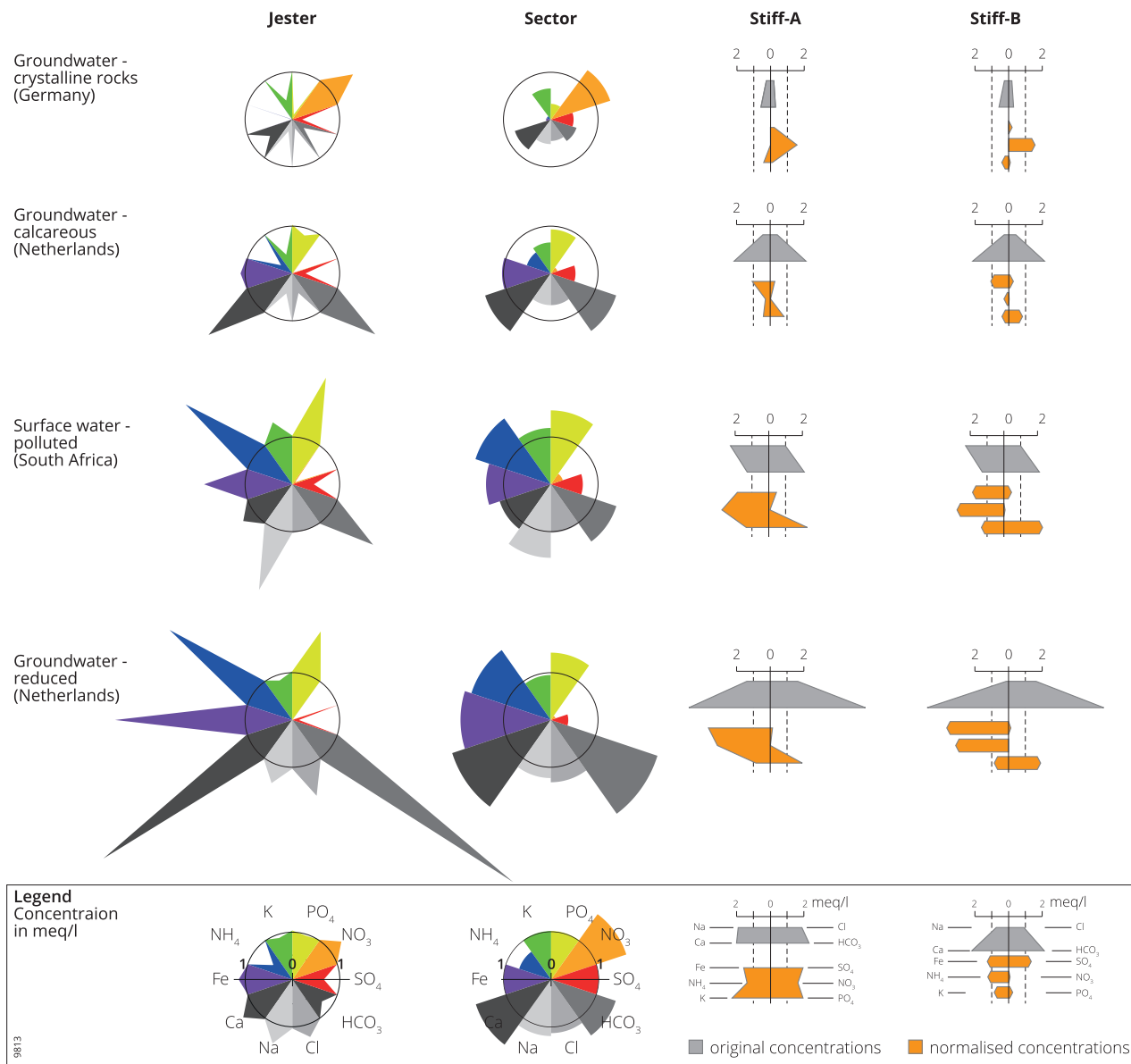


Fig. 5. Comparison of the 4 adapted water quality diagrams for a number of samples from the regional, national, continental and temporal databases used above.

NH<sub>4</sub>, phosphorus as PO<sub>4</sub>, and K as a separate variable. Nitrate has been used in some variations of the classical Stiff diagram (eg. Nyenje et al., 2013) but not regularly. Potassium is included in the Piper, and often in Stiff diagrams, as a summed value of Na + K, but never as separate value. Ammonium and PO<sub>4</sub> are not used at all in classical water quality diagrams. The only known exception is an adapted Stiff diagram by Wassen et al. (1988) showing separate concentrations of NO<sub>3</sub>, NH<sub>4</sub> and PO<sub>4</sub> as three additional separate lines, but the diagram lacked a clear shape to discern and characterize different water types. Therefore, the adapted water quality diagrams presented may be considered as a response to the plea made by Pedroli (1990) for an internationally applicable composite classification adapted to ecohydrological research.

Finally, using policy norms for scaling of ions has the advantage of providing an ‘alarm function’ of exceedance of norms, i.e. when concentrations surpass the ring in the diagram (Fig. 2b and 4b). We could not find any published application to the Stiff or Maucha diagrams. Such alarm functions may be useful in monitoring efforts on local, regional or even continental scale, e.g. in light of the EU Water Framework Directive.

A number of choices were made during the creation of the adapted

diagrams. First, the number of selected water quality parameters has been a trade-off between supplying as much information as possible, and keeping the number of parameters low enough to retain a comprehensible diagram. We used 10 parameters to define our diagrams. This is somewhat higher than the classical diagrams that commonly use between 6 and 8 parameters. We have tried to facilitate interpretation of the Stiff-A and Stiff-B diagrams by using different colours for the macro-ions (grey) and the minor ions (orange). For the Jester and Sector we used grey tones for the macro-ions and different bright colours for each minor ion emphasizing our focus on ecohydrological purposes.

Next, the choice for a diagram form was not that unequivocal as initially envisaged. Although we initially aimed at defining only one adapted diagram, discussions with multiple colleagues led to the insight that form preferences may differ between different people, for all sorts of reasons. This led to the decision not to try to devise one type of diagram, but to present multiple diagram forms from which professionals may pick their own favorite. By presenting multiple forms we have tried to make available a set of diagrams based on the same assumptions as to the ions to be included, but different appearances that may suit different needs and preferences. Likewise we presented two forms of scaling of

minor ions, based on average concentrations or on policy norms. Time will tell which forms and scaling will be applied, and for what kind of specific applications or reasons.

An important point of discussion pertains to the scaling of the minor ions. We examined both using average and using median values of the 6 selected minor ions as a basis for scaling. It appeared average values presented visually more informative diagrams than median values. This is probably due to the skewed distribution of most minor ions which often display many values below or just above the detection limit. This implies median concentrations may be relatively low, leading to high scaling factors and subsequent extreme long points or bars in the diagrams for samples that are well above the median concentrations. By using averages as a basis for scaling there are much less extremes.

The choice of using averages of concentrations for the minor ions has another important implication. By using averages of concentrations found in a certain dataset the scaling basically becomes dataset- or area-specific. Since concentrations found in area A may be significantly different from those in area B, the resulting average concentrations per area will also differ. This then leads to different scaling factors per minor ion per area. This implies that diagrams as to the minor ions are basically incomparable between different datasets of different areas. For the macro-ions they are in principle comparable as these are displayed by their true concentration in meq/l, although the scaling of the meq/l axes may still differ between areas depending on the maximum values observed per area.

Even within the same area one should consider what averages to use. When sampling occurs at different moments in time (e.g. for monitoring), two approaches can be followed. Either one keeps the scaling based on the first sampling, in which case concentrations of new samples can be directly compared with the old samples (as scaling is the same), in terms of increased/decreased concentrations over time. Another approach is to calculate averages for each minor ion based on the complete dataset of all samplings over time, and then scale samples of each monitoring event relative to these overall averages. As long as the same scaling is used for different moments in time, old and new samples can be directly compared.

To enable 1:1 comparison of the diagrams between datasets from different areas a uniform scaling of the minor ions should be applied. We tried to find such a scaling based on comparing ranges and averages of different datasets from different areas within The Netherlands and within Europe. We could however not find a one-size-fits-all scaling method per parameter. This is because different (geological) areas have different water quality characteristics, with different average concentrations, and thus different optimal scaling factors. We tried to determine a sort of 'average' overall scaling factor for each minor ion that could be applied uniformly for all areas. This however had too much of a compromising effect on the information value of the diagrams per specific area. We therefore decided to use area specific scaling factors. There are simply too many differences between areas with respect to the different minor ion concentrations as a result of differences in geology, human interventions, etc.

A similar effect occurs when water quality norms are used for scaling of minor ions, since water quality norms may differ per country or area considered. They also differ between policy fields or intended use, e.g. different norms for drinking water, industrial use, or natural ecosystems. For example the ecohydrological standards for  $\text{NO}_3$  are much lower than e.g. the drinking water limit of 50 mg/L of the European Union. Moreover, depending on the type of ecosystem one is aiming to protect or restore, different nitrate concentrations may be relevant depending on the tolerance of specific ecosystems to nitrates. Similarly the norms for other water quality parameters may differ between ecosystem types, e.g. bogs need acidic, oligotrophic water while fens need more alkaline, mesotrophic water. The same obviously applies to all other minor ions. Comparability of diagrams based on policy norms between different areas therefore necessitates a uniform norm, e.g. the EU drinking water standard of 50 mg/l for nitrate.

Our adapted water quality diagrams were devised to be used by researchers and water managers alike. We offer free access to our codes which enables users to modify them when needed, e.g. add or replace certain parameters that are of particular interest to them. We are curious to see which of the adapted ecohydrological water quality diagrams will be applied in future studies, and whether a more uniform scaling of (part of) the minor ions will develop.

Note on accessing diagram plotting scripts.

The code used to plot the adapted diagrams is openly accessible and freely usable by the community at large. Your own data can be inputted into a data entry sheet and plotted by running a single-click R script. The R project featuring code and data entry sheet is available at the following location:

<https://github.com/jebeard/WaterType-Diagrams>.

## 5. Conclusion

This paper sets out to present water quality diagrams that are relevant for ecohydrological research and related policy applications. Classical water quality diagrams being mainly developed for geo-hydrological purposes miss comprehensive information on nutrients which is pivotal to ecological functioning. Ecological considerations are on the forefront of present day policy efforts directed at achieving sustainable development, which results in associated information needs.

We developed water quality diagrams which include all four ecohydrologically relevant nutrient species ( $\text{NO}_3$ ,  $\text{NH}_4$ ,  $\text{PO}_4$ , K). The diagrams largely retain the traditional information on ions for hydrogeological characterization and additionally offer advanced insight in redox status from the combination of four redox-sensitive parameters (Fe,  $\text{NO}_3$ ,  $\text{SO}_4$ ,  $\text{NH}_4$ ). For ions that usually make up the bulk of the dissolved solids (Na, Cl, Ca,  $\text{HCO}_3$ ) concentrations are displayed in absolute meq/l. For the ions that are usually less dominant in meq/l ( $\text{NO}_3$ ,  $\text{NH}_4$ ,  $\text{PO}_4$ , K, Fe,  $\text{SO}_4$ ) the concentrations can be scaled in two ways: 1) Relative to the average concentration of the ion at hand for the given dataset, with the average plotted at 1 meq/l; 2) Relative to an established policy norm for the minor ion (eg. nutrients or iron), with the norm plotted at 1 meq/l.

The diagrams may be used to compare water quality samples in a spatial mode or a temporal mode. Depending on the chosen scaling of the redox-sensitive ions and nutrients, the diagrams show at what location or time their concentrations are higher resp. lower than the average concentration, or than the policy norm concentration set for a particular ion parameter.

Four different diagram appearances are developed on the basis of classical Maucha and Stiff diagrams. The Stiff-A diagram resembles the classical Stiff diagram with connection lines between the concentrations of the different ions. This gives them a characteristic form that may be attributed to certain water quality types. Stiff-B diagrams present concentrations as bars making it somewhat easier to distinguish separate (relative) concentrations. Jester diagrams have a pronounced spiky form that highlights large (relative) concentrations of samples. The Sector diagrams are more condensed showing a less outpointing appearance than the Jester.

We envisage application of scaling to averages amongst ecohydrological researchers to highlight the main differences in an area or timeframe. Scaling relative to norms is likely more relevant for policy makers and evaluation of routine monitoring efforts. Policy norms scaling has the advantage of providing an 'alarm function' of exceedance of norms, eg. those used for the EU Water Framework Directive.

We made our R-scripts publicly available which enables users to modify the R-script to their particular needs.

## CRedit authorship contribution statement

**Paul Schot:** Conceptualization, Methodology, Investigation, Writing – original draft, Writing – review & editing, Supervision. **Jack Beard:**

Software, Visualization. **Riki Hissink:** Software, Validation. **Michael Silberbauer:** Investigation, Writing – review & editing, Visualization, Software. **Jasper Griffioen:** Investigation, Writing – review & editing.

### Declaration of Competing Interest

The authors declare that they have no known competing financial interests or personal relationships that could have appeared to influence the work reported in this paper.

### Data availability

Data will be made available on request.

### References

- Appelo, C.A.J., Postma, D., 2004. *Geochemistry, Groundwater and Pollution*. CRC Press.
- Appelo, C.A.J., Willemssen, A., 1987. Geochemical calculations and observations on salt water intrusions. I A combined geochemical/mixing cell model. *J. Hydrol.* 94 (3–4), 313–330.
- Avnimelech, Y., 1980. Calcium-carbonate-phosphate surface complex in calcareous systems. *Nature* 288 (5788), 255–257.
- Boudsocq, S., Niboyet, A., Lata, J.C., Raynaud, X., Loeuille, N., Mathieu, J., Blouin, M., Abbadie, L., Barot, S., 2012. Plant preference for ammonium versus nitrate: a neglected determinant of ecosystem functioning? *Am. Nat.* 180 (1), 60–69.
- Broch, E.S., Yake, W., 1969. A modification of Maucha's ionic diagram to include ionic concentrations. *Limnol. Oceanogr.* 14 (6), 933–935.
- Cloutier, V., Lefebvre, R., Therrien, R., Savard, M.M., 2008. Multivariate statistical analysis of geochemical data as indicative of the hydrogeochemical evolution of groundwater in a sedimentary rock aquifer system. *J. Hydrol.* 353 (3–4), 294–313.
- Collins, W.D., 1923. Graphic representation of analyses. *Ind. Eng. Chem.* 15, 394.
- Cowx, I.G., Arlinghaus, R., Cooke, S.J., 2010. Harmonizing recreational fisheries and conservation objectives for aquatic biodiversity in inland waters. *J. Fish Biol.* 76 (9), 2194–2215.
- Dieperink, C., 2000. Successful international cooperation in the Rhine catchment area. *Water Int.* 25 (3), 347–355.
- Directive, W.F. (2000). Water Framework Directive. Journal reference OJL, 327, 1-73.
- Dodds, W.K., Bouska, W.W., Eitzmann, J.L., Pilger, T.J., Pitts, K.L., Riley, A.J., Schloesser, J.T., Thornbrugh, D.J., 2009. Eutrophication of U.S. Freshwaters: analysis of potential economic damages. *Environ. Sci. Technol.* 43 (1), 12–19.
- Domenico, P.A., Schwartz, F.W., 1998. *Physical and Chemical Hydrogeology*, 2nd Edition. Wiley, New York.
- Drever, J.I., 1997. *The Geochemistry of Natural waters*, 3rd Ed. Prentice-Hall, Englewood Cliffs.
- Drinkwaterbesluit, 2011. Drinkwaterbesluit (Drinking water act), Rijksoverheid (National Dutch government) 2011. Available at: <https://wetten.overheid.nl/BWB-R0030111/2011-07-01>. Accessed 11-2-2022.
- Dunne, E.J., Reddy, K.R., 2005. Phosphorus biogeochemistry of wetlands in agricultural watersheds. In: *Nutrient Management in agricultural Watersheds: a Wetland Solution*. Wageningen Academic Publishers, Wageningen, The Netherlands, pp. 105–119.
- DWAF (1996). *South African Water Quality Guidelines. Volume 8: Field Guide. Second edition. Department of Water Affairs and Forestry, Pretoria, South Africa. 58pp. Available at: https://www.dws.gov.za/iwqs/wq\_guide/edited/Pol\_saWQguideFRESH\_vol8\_Fieldguide.pdf. Accessed 11-2-2022.*
- DWS (2016). Schedule: classes and resource quality objectives of water resources for catchments of the Upper Vaal in terms of section 13(1)(a) and (b) of the National Water Act (Act no.36 of 1998). National Water Act. Department of Water and Sanitation, Pretoria, South Africa. Available at: <https://cer.org.za/wp-content/uploads/2010/05/Upper-Vaal.pdf>. Accessed 11-2-2022.
- Dzwairo, B., Otieno, F.A.O., 2014. Chemical pollution assessment and prioritisation model for the Upper and Middle Vaal water management areas of South Africa. *J. Water Health* 12 (4), 803–816.
- Ertsen, A.C.D., Alkemade, J.R.M., Wassen, M.J., 1998. Calibrating Ellenberg indicator values for moisture, acidity, nutrient availability and salinity in the Netherlands. *Plant Ecol.* 135 (1), 113–124.
- Frapporti, G., Friend, S.P., Van Gaans, P.F.M., 1993. Hydrogeochemistry of the shallow Dutch groundwater: interpretation of the national Groundwater Quality Monitoring Network. *Water Resour. Res.* 29 (9), 2993–3004.
- Freeze, R.A., Cherry, J.A., 1979. *Groundwater*. Prentice-Hall, Englewood Cliffs, New Jersey, p. 604.
- Gächter, R., Müller, B., 2003. Why the phosphorus retention of lakes does not necessarily depend on the oxygen supply to their sediment surface. *Limnol. Oceanogr.* 48 (2), 929–933.
- Gorham, E., Eisenreich, S.J., Ford, J., Santelmann, M.V., 1985. Chemistry of bog waters. In: *Chemical Processes in Lakes*. John Wiley and Sons, pp. 339–362.
- Griffioen, J., 2006. Extent of immobilisation of phosphate during aeration of nutrient-rich, anoxic groundwater. *J. Hydrol.* 320 (3–4), 359–369.
- Griffioen, J., Passier, H.F., Klein, J., 2008. Comparison of selection methods to deduce natural background levels for groundwater units. *Environ. Sci. Technol.* 42 (13), 4863–4869.
- Griffioen, J., Vermooten, S., Janssen, G., 2013. Geochemical and palaeohydrological controls on the composition of shallow groundwater in the Netherlands. *Appl. Geochem.* 39, 129–149.
- Hannah, D.M., Wood, P.J., Sadler, J.P., 2004. Ecohydrology and hydroecology: a 'new paradigm'? *Hydrol. Process.* 18 (17), 3439–3445.
- Heffing, M., Clément, J.C., Dowrick, D., Cosandey, A.C., Bernal, S., Cimpian, C., Tatur, A., Burt, T.P., Pinay, G., 2004. Water table elevation controls on soil nitrogen cycling in riparian wetlands along a European climatic gradient. *Biogeochemistry* 67 (1), 113–134.
- Heikkinen, P.M., Räisänen, M.L., Johnson, R.H., 2009. Geochemical characterisation of seepage and drainage water quality from two sulphide mine tailings impoundments: acid mine drainage versus neutral mine drainage. *Mine Water Environ.* 28 (1), 30–49.
- Herbert, E.R., Boon, P., Burgin, A.J., Neubauer, S.C., Franklin, R.B., Ardón, M., Hopfensperger, K.N., Lamers, L.P.M., Gell, P., 2015. A global perspective on wetland salinization: ecological consequences of a growing threat to freshwater wetlands. *Ecosphere* 6 (10), art206.
- House, W.A., Denison, F.H., 2002. Total phosphorus content of river sediments in relationship to calcium, iron and organic matter concentrations. *Sci. Total Environ.* 282, 341–351.
- Jeong, C.H., 2001. Effect of land use and urbanization on hydrochemistry and contamination of groundwater from Taejon area, Korea. *J. Hydrol.* 253 (1–4), 194–210.
- Kumar, M., Ramanathan, A.L., Rao, M.S., Kumar, B., 2006. Identification and evaluation of hydrogeochemical processes in the groundwater environment of Delhi, India. *Environ. Geol.* 50 (7), 1025–1039.
- Kundzewicz, Z.W., 2002. Ecohydrology—seeking consensus on interpretation of the notion/Ecohydrologie—à la recherche d'un consensus sur l'interprétation de la notion. *Hydrol. Sci. J.* 47 (5), 799–804.
- Lamers, L.P., Tomassen, H.B., Roelofs, J.G., 1998. Sulfate-induced eutrophication and phytotoxicity in freshwater wetlands. *Environ. Sci. Technol.* 32 (2), 199–205.
- Magaritz, M., Luzier, J.E., 1985. Water-rock interactions and seawater-freshwater mixing effects in the coastal dunes aquifer, Coos Bay, Oregon. *Geochimica et Cosmochimica Acta* 49 (12), 2515–2525.
- Martínez, D., Bocanegra, E., 2002. Hydrogeochemistry and cation-exchange processes in the coastal aquifer of Mar Del Plata, Argentina. *Hydrogeol. J.* 10 (3), 393–408.
- Mastrocicco, M., Giambastiani, B.M.S., Colombani, N., 2013. Ammonium occurrence in a salinized lowland coastal aquifer (Ferrara, Italy). *Hydrol. Process.* 27 (24), 3495–3501.
- Mateo-Sagasta, J., Zadeh, S.M., Turrall, H., Burke, J. (2017). *Water pollution from agriculture: a global review. Executive summary. Food and Agriculture Organization of the United Nations, Rome and the International Water Management Institute, Colombo, 2017.*
- Mattson, M.D., Likens, G.E., 1992. Redox reactions of organic matter decomposition in a soft water lake. *Biogeochemistry* 19 (3), 149–172.
- Maucha R. In: Thienemann A, editor. *Hydrochemische Methoden in der Limnologie XII. Stuttgart: Schweizerbart; 1932. p. 1-173.*
- Millennium Ecosystem Assessment, 2005. *Ecosystems and Human Well-Being: Wetlands and Water Synthesis*. World Resources Institute, Washington, DC.
- Naus, F.L., Schot, P., Groen, K., Ahmed, K.M., Griffioen, J., 2019. Groundwater salinity variation in Upazila Assasuni (southwestern Bangladesh), as steered by surface clay layer thickness, relative elevation and present-day land use. *Hydrol. Earth Syst. Sci.* 23 (3), 1431–1451.
- Nyenje, P.M., Foppen, J.W., Kulabako, R., Muwanga, A., Uhlenbrook, S., 2013. Nutrient pollution in shallow aquifers underlying pit latrines and domestic solid waste dumps in urban slums. *J. Environ. Manage.* 122, 15–24.
- Pedroli, B., 1990. Ecohydrological parameters indicating different types of shallow groundwater. *J. Hydrol.* 120 (1–4), 381–404.
- Piper, A.M., 1944. A graphic procedure in the geochemical interpretation of water-analyses. *Eos, Trans. Am. Geophys. Union* 25 (6), 914–928.
- Porporato, A., Rodriguez-Iturbe, I., 2002. Ecohydrology—a challenging multidisciplinary research perspective/Ecohydrologie: une perspective stimulante de recherche multidisciplinaire. *Hydrol. Sci. J.* 47 (5), 811–821.
- Post, V.E.A., 2004. *Groundwater salinization processes in the coastal area of the Netherlands due to transgressions during the Holocene*. Free University Amsterdam. PhD Thesis.
- Prol-Ledesma, R.M., Canet, C., Torres-Vera, M.A., Forrest, M.J., Armentia, M.A., 2004. Vent fluid chemistry in Bahía Concepción coastal submarine hydrothermal system, Baja California Sur, Mexico. *J. Volcanol. Geoth. Res.* 137 (4), 311–328.
- Rosset, V., Angélibert, S., Arthaud, F., Bornette, G., Robin, J., Wezel, A., Vallod, D., Oertli, B., Arnott, S., 2014. Is eutrophication really a major impairment for small waterbody biodiversity? *J. Appl. Ecol.* 51 (2), 415–425.
- Schoeller, 1955. *Géochimie des eaux souterraines*. Revue de l'Institut Français de Pétrole 10, 230–244.
- Schot, P.P., 1990. Groundwater systems analysis of the Naardermeer wetland, the Netherlands. Selected Papers on Hydrogeology From the 28th International Geological Congress.
- Schot, P.P., Barendregt, A., Wassen, M.J., 1988. Hydrology of the wetland Naardermeer: influence of the surrounding area and impact on vegetation. *Agric. Water Manag.* 14 (1–4), 459–470.
- Schot, P.P., Molenaar, A., 1992. Regional changes in groundwater flow patterns and effects on groundwater composition. *J. Hydrol.* 130 (1–4), 151–170.
- Schot, P.P., Van der Wal, J., 1992. Human impact on regional groundwater composition through intervention in natural flow patterns and changes in land use. *J. Hydrol.* 134 (1–4), 297–313.

- Schot, P.P., Wassen, M.J., 1993. Calcium concentrations in wetland groundwater in relation to water sources and soil conditions in the recharge area. *J. Hydrol.* 141 (1–4), 197–217.
- Schot, P.P., Dekker, S.C., Poot, A., 2004. The dynamic form of rainwater lenses in drained fens. *J. Hydrol.* 293 (1–4), 74–84.
- Showalter, P.S., Silberbauer, M., Moolman, J., Howman, A., 2000. Revisiting Rietspruit: Land Cover Change and Water Quality in South Africa. In: *Proceedings of the ICRSE 28th International Symposium on Remote Sensing of Environment and the Third AARSE Symposium*. Cape Town, South Africa.
- Silberbauer, M.J., 2009. Methods for visualising complex water quality data. University of Cape Town, South Africa. PhD Thesis.
- Silberbauer, M., 2011. Multivariate Point Data Visualisation - Geographical information Systems Developments to Aid in Water Quality Management. AGILE, Utrecht, the Netherlands.
- Silberbauer, M.J., King, J.M., 1991. Geographical trends in the water chemistry of wetlands in the south-western Cape Province, South Africa. *Southern Afr. J. Aquat. Sci.* 17 (1–2), 82–88.
- Silberbauer, M.J., Moolman, J., 1993. Changes in urban residential land in the Rietspruit catchment, southern Transvaal. *Southern Afr. J. Aquat. Sci.* 19 (1/2), 89–94.
- Smolders, A.J.P., Lamers, L.P.M., Lucassen, E.C.H.E.T., Van der Velde, G., Roelofs, J.G. M., 2006. Internal eutrophication: how it works and what to do about it—A review. *Chem. Ecol.* 22 (2), 93–111.
- Sommerwerk, N., Bloesch, J., Paunović, M., Baumgartner, C., Venohr, M., Schneider-Jacoby, M., Hein, T., Tockner, K., 2010. Managing the world's most international river: the Danube River Basin. *Mar. Freshw. Res.* 61 (7), 736.
- Stiff, H.A. 1951. *The interpretation of chemical water analysis by means of patterns*. *J. Petrol. Technol.* 3:sec.1, 15-16-sec.2, 3.
- Stuyfzand, P.J. (1988). De alkaliteit, het redoxniveau en de verontreinigingsindex als parameters en keuzemogelijkheden in een hydrochemische classificatie van watertypen. *H2O*, 21, 640-643.
- Stuyfzand, P.J., 1993. Hydrochemistry and hydrology of the coastal dune area of the Western Netherlands. VU (Free University), Amsterdam. PhD Thesis.
- Subramani, T., Elango, L., Damodarasamy, S.R., 2005. Groundwater quality and its suitability for drinking and agricultural use in Chithar River Basin, Tamil Nadu, India. *Environ. Geol.* 47 (8), 1099–1110.
- Van Beek, C.G.E.M., Puffelen, V.J., 1987. Changes in the chemical composition of drinking water after well infiltration in an unconsolidated sandy aquifer. *Water Resour. Res.* 23 (1), 69–76.
- Van Den Brink, C., Frapporti, G., Griffioen, J., Zaadnoordijk, W.J., 2007. Statistical analysis of anthropogenic versus geochemical-controlled differences in groundwater composition in The Netherlands. *J. Hydrol.* 336 (3–4), 470–480.
- Van Loon, A.H., Schot, P.P., Griffioen, J., Bierkens, M.F.P., Batelaan, O., Wassen, M.J., 2009. Throughflow as a determining factor for habitat contiguity in a near-natural fen. *J. Hydrol.* 379 (1–2), 30–40.
- Van Wirdum, G., 1991. Vegetation and hydrology of floating rich-fens. University of Amsterdam, Datawysse, Maastricht, The Netherlands. PhD Thesis.
- Wassen, M.J., Barendregt, A., Bootsma, M.C., Schot, P.P., 1988. Groundwater chemistry and vegetation of gradients from rich fen to poor fen in the Naardermeer (the Netherlands). *Vegetatio* 79 (3), 117–132.
- Wassen, M.J., Barendregt, A., Schot, P.P., Beltman, B., 1990. Dependency of local mesotrophic fens on a regional groundwater flow system in a poldered river plain in the Netherlands. *Landscape Ecol.* 5 (1), 21–38.
- Wendland, F., Blum, A., Coetsiers, M., Gorova, R., Griffioen, J., Grima, J., Hinsby, K., Kunkel, R., Marandi, A., Melo, T., Panagopoulos, A., Pauwels, H., Ruisi, M., Traversa, P., Vermooten, J.S.A., Walraevens, K., 2008. European aquifer typology: a practical framework for an overview of major groundwater composition at European scale. *Environ. Geol.* 55 (1), 77–85.
- Yidana, S.M., Banoeng-Yakubo, B., Akabzaa, T.M., 2010. Analysis of groundwater quality using multivariate and spatial analyses in the Keta basin, Ghana. *J. Afr. Earth Sci.* 58 (2), 220–234.
- Zalewski, M., 2000. Ecohydrology-the scientific background to use ecosystem properties as management tools toward sustainability of water resources. *Ecol. Eng.* 16 (1), 1–8.
- Zhang, Y.C., Slomp, C.P., Broers, H.P., Passier, H.F., Van Cappellen, P., 2009. Denitrification coupled to pyrite oxidation and changes in groundwater quality in a shallow sandy aquifer. *Geochim. Cosmochim. Acta* 73 (22), 6716–6726.